

$Tb_2Ti_2O_7$: a 'spin liquid' single crystal studied under high pressure and high magnetic field

This article has been downloaded from IOPscience. Please scroll down to see the full text article.

2005 J. Phys.: Condens. Matter 17 S771

(<http://iopscience.iop.org/0953-8984/17/11/005>)

View [the table of contents for this issue](#), or go to the [journal homepage](#) for more

Download details:

IP Address: 129.252.86.83

The article was downloaded on 27/05/2010 at 20:30

Please note that [terms and conditions apply](#).

Tb₂Ti₂O₇: a ‘spin liquid’ single crystal studied under high pressure and high magnetic field

I Mirebeau¹ and I N Goncharenko

Laboratoire Léon Brillouin CE-Saclay, 91191 Gif sur Yvette, France

E-mail: imirebeau@cea.fr

Received 5 January 2005

Published 4 March 2005

Online at stacks.iop.org/JPhysCM/17/S771

Abstract

Tb₂Ti₂O₇ is a very intriguing case of a geometrically frustrated compound where the short range correlated moments still fluctuate down to extremely low temperatures. We studied this compound by means of single-crystal neutron diffraction for an unprecedented range of thermodynamical parameters combining high pressures (up to 2.8 GPa), high magnetic fields (up to 7 T) and low temperatures (down to 0.14 K). We also investigated the effects of several conditions: a hydrostatic pressure, a uniaxial stress and a combination of the two. We show that a long range antiferromagnetic phase can be induced under pressure. The Néel temperature and the ordered magnetic moment may be tuned by means of the direction of the anisotropic pressure component. Under an applied field, the antiferromagnetic structure transforms into a non-collinear ferromagnetic one at a low field of 0.3 T; then the spin canting persists up to very high fields (above 7 T). Thermal and field hysteresis phenomena are observed at low fields and low temperatures. We show the pressure and magnetic field magnetic phase diagram deduced from our data. We also present microscopic models for the neutron correlations deduced from a refinement of the neutron intensities, using both symmetry analysis and simulated annealing processes. We discuss the implications of these results for the understanding of the mysterious spin liquid phase stabilized at ambient pressure.

1. Introduction

1.1. Classical and quantum spin liquids

Among liquids, the only one which remains liquid down to $T = 0$ is helium, due to zero-point motion and quantum fluctuations. In magnetism, some systems also remain in an unusual state of short range correlated fluctuating spins down to very low temperatures, well below the

¹ Author to whom any correspondence should be addressed.

Curie–Weiss temperature which sets the scale of the magnetic exchange interactions. They have been called ‘spin liquids’ and, actually, the Fourier transform of the spin correlations is quite similar to the pair correlation function of a casual liquid. How can such a spin liquid state be stable? The main requirement is to suppress the transition towards long range magnetic order. This can be realized in some peculiar cases, e.g. low dimensional systems such as the Haldane chain, spin ladders and 2D spin dimer systems [1], the nuclear quantum magnet ^3He where the pairwise exchange interactions are replaced by multiple exchange interactions [2] and the wide class of geometrically frustrated magnets. A spin liquid state could be expected in strongly correlated electron systems with low spin values, and may be the precursor of or an alternative to unconventional superconductivity [3]. In the last few years a considerable theoretical effort was made to investigate $S = 1/2$ Heisenberg spins on 2D and 3D frustrated lattices, yielding predictions of exotic phases such as the spin liquid resonating valence bond (RVB) state and the valence bond crystal [4, 5], as well as new kinds of spin or spin charge excitations such as confined spinons, or low lying excitations in the gap between the singlet ground state and the first excited state. Enhancement of hole pairing in frustrated lattices was predicted [6]. The recent discovery of superconductivity in frustrated lattices such as the $\text{Na}_x\text{CoO}_2 \cdot y\text{H}_2\text{O}$ compounds with triangular layers [7] and the $\text{Cd}_2\text{Re}_2\text{O}_7$ and KOs_2O_6 pyrochlores [8], and the heavy fermion behaviour of the frustrated spinel LiV_2O_4 [9], have revived this interest further.

The Kagome (2D) and pyrochlore (3D) lattices offer the best examples of geometrically frustrated lattices (GFM) with low connectivity, favouring the occurrence of a spin liquid state. In the pyrochlore lattice, a non-ordered ground state is predicted for Heisenberg spins with first-neighbour antiferromagnetic interactions, both in the classical mean field approximation [10] and in quantum models [11]. Experimentally, the pyrochlore compounds offer a huge variety of magnetic behaviours, more or less close to theoretical predictions. Localized excitations were observed in the Cr spinels with the pyrochlore lattice [12]. In other frustrated spinels, the interplay of orbital, lattice and magnetic degrees of freedom was recently observed [13], and could be connected with the formation of spin singlets [14]. High field magnetization plateaus were observed in several pyrochlores [15, 16]. However, no true realization of the quantum liquid state predicted by theory has been confirmed so far. In real systems, any energy perturbation may destroy the stability of the spin liquid state. It may have various origins such as further neighbour exchange, anisotropy, dipolar interactions, chemical and bond disorder. Thermal or quantum fluctuations may also relieve the degeneracy of the ground state by selecting a particular state in an order-by-disorder process. Finally, most systems order in complex AF or spin glass phases [17], at a T_C value well below the Curie–Weiss temperature θ_{CW} , the ratio $f = |\theta_{\text{CW}}/T_C|$ measuring the strength of the frustration.

1.2. The mysterious case of $\text{Tb}_2\text{Ti}_2\text{O}_7$

The pyrochlore compound $\text{Tb}_2\text{Ti}_2\text{O}_7$ offers a very intriguing case of a spin liquid state stabilized for large classical spins, down to 70 mK at least, that is well below the energy scale set by the Curie–Weiss temperature of -19 K (f around 300). The compound shows perfect chemical order [18]. The spin fluctuations probed by inelastic neutron scattering and muon spin resonance [19, 20] slow down below 1.5 K, leading to irreversibilities in the magnetization below about 0.2 K [21, 22], and anomalies in the specific heat in the same temperature range [22]. These recent results suggest that a spin glass or cluster glass state coexists with the spin liquid fluctuations below 0.2 K. It is usually admitted that the single-ion ground state (GS) of the Tb^{3+} spin is a degenerate doublet, separated from the first excited state by a low energy gap of 18 K, although the wavefunctions associated with the

energy levels remain controversial [20, 23, 24]. Theoretical models taking dipolar, anisotropy and exchange interactions into account [25, 26] lead to predictions of a transition towards a $\mathbf{k} = 0$ antiferromagnetic state at 2.1 K, in contrast with experiment. Very probably, quantum fluctuation within the GS and between the GS and the first excited state play a crucial role in this enigma. The peculiar crystal field scheme, which is at the origin of the giant magnetostriction [23], suggests a strong coupling between spin and lattice degrees of freedom, which could offer a way to relieve the frustration.

Recently, we managed to induce long range magnetic order in Tb₂Ti₂O₇ by applying a quasihydrostatic pressure [27, 28]. The pressure induced order was observed by means of powder neutron diffraction up to 8.6 GPa. A complex antiferromagnetic structure was found, coexisting with the spin liquid phase down to the lowest temperature measured (1.4 K). These experiments opened new possibilities for playing with the complex energy balance with controls the stability of these systems, but also raised several crucial questions: What is the exact magnetic structure? What is the role of pressure? What is the ground state?

To answer these questions, we have now performed new measurements on single crystals, down to very low temperatures (0.14 K), and studied several pressure conditions. We also studied the combined effect of an applied pressure and a high magnetic field (up to 7 T), which induces a new magnetic phase. These experiments realize a unique combination of three extreme conditions, which allows us to understand better and therefore to control the competition between liquid and ordered states. We report them below. A shorter account of these results is given in [29].

2. Experimental details

A large single crystal was grown by the flux zone method. Its structure, of space group $Fd\bar{3}m$, was checked on the neutron four-circle diffractometer 5C1 at the LLB, showing full chemical order and oxygen stoichiometry within the accuracy of the measurement (0.5%). Thin plates from 1 to 0.15 mm thickness and 1 mm² surface were cut perpendicular to the principal axes [111], [100] or [110] of the cubic cell. The sample was inserted in a Kurchatov–LLB pressure cell [30]. By choosing the appropriate transmitting medium we were able to impose either a uniaxial stress (no transmitting medium) or a hydrostatic pressure (liquid ethanol–methanol transmitting medium), or a combination of the two (NaCl solid transmitting medium). Pressure was measured by the ruby fluorescence technique. Its anisotropic component was estimated on the G6-1 diffractometer of LLB by measuring the positions of the diffraction peaks for different orientations of the pressure cell [30]. The cell was fixed at the end of a ³He–⁴He dilution insert tube, inside a superconducting coil. The measurements were performed on the single-crystal diffractometer 6T2 of the LLB with a lifting arm with an incident neutron wavelength of 2.34 Å.

3. A magnetic order tuned by pressure

We first checked the influence of a hydrostatic pressure $P_i = 2.8$ GPa, down to 0.14 K (figure 1, top right). The structural (440) peak is clearly seen, but no intensity appears at the expected position of AF peaks of the magnetic structure, which means that no long range magnetic order is induced in this configuration. Then we checked the effect of a uniaxial pressure or stress P_u , applied along either the [111] or the [110] crystal direction. We applied a stress of 0.3 GPa, which is the upper limit for keeping the single crystal. Intense (440)-type peaks are observed, whose split shows that the crystal starts to be damaged under stress. In this case

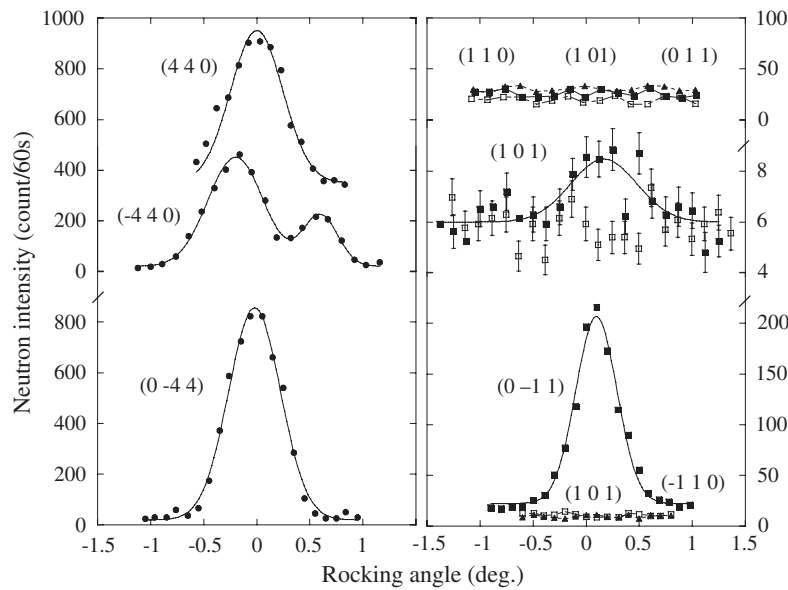


Figure 1. Nuclear (left) and magnetic (right) peaks at 0.14 K in $\text{Tb}_2\text{Ti}_2\text{O}_7$ for three typical pressure configurations. Top: isotropic pressure $P_1 = 2.8$ GPa. Middle: isotropic pressure $P_1 = 2.0$ GPa and uniaxial pressure $P_u = 0.3$ GPa along the [111] axis. Bottom: isotropic pressure $P_1 = 2.4$ GPa and uniaxial pressure $P_u = 0.3$ GPa along the [011] axis. The background intensities (middle right) are measured at temperatures above the Néel transition. The extinctions at specific peaks positions (bottom right) show that the magnetic structure is a single-domain and single-k structure.

as well, we did not find any magnetic order, at least down to 1.4 K. Finally, by combining hydrostatic and uniaxial pressure components, we clearly observed the AF peaks of the simple cubic structure. Their intensity strongly depends on the direction of the applied stress. When P_u is oriented along the [111] axis, a very weak intensity is observed in the (101) peak (figure 1, middle). With P_u oriented along the [011] axis (figure 1, bottom), an intense magnetic signal appears at the (0 $\bar{1}$ 1) peak, increased by about a factor 30 with respect to the previous case. The complete results suggest that both isotropic and anisotropic components are needed to induce long range magnetic order, and that the anisotropy direction controls the magnitude of the ordered moment. The Néel temperature can also be tuned by means of the uniaxial stress. With $P_u = 0.3$ GPa applied along the [111] axis, T_N has a low value of 0.7(1) K (figure 2(a)). In contrast, with P_u along the [011] axis, T_N is strongly enhanced to the value of 1.78(5) K (figure 2(b)).

4. Pressure and magnetic field

When a magnetic field is applied along the [011] axis of the uniaxial pressure gradient, one observes strong changes of the magnetic peaks, which characterize the onset of a new magnetic phase (figures 3 and 4). The AF peaks of the simple cubic structure disappear at low fields. Concomitantly, a magnetic contribution appears in the fcc peaks of the structural lattice. These changes correspond to a transition from an antiferromagnetic structure with propagation vector $\mathbf{k} = (1, 0, 0)$ to another structure with $\mathbf{k} = 0$, most probably with ferromagnetic or ferrimagnetic character. The (002) peak intensity strongly increases at low fields, then shows a broad maximum at intermediate field values and starts to decrease very slowly at high fields

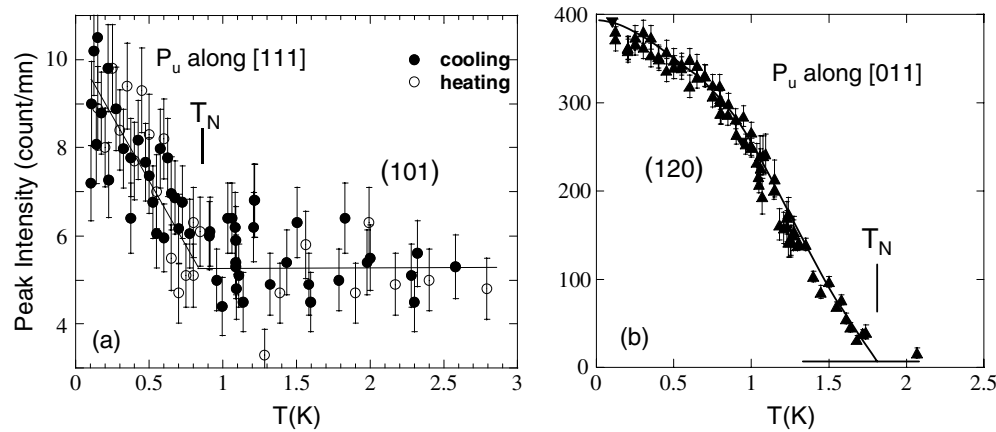


Figure 2. Tb₂Ti₂O₇. A Néel transition tuned by means of uniaxial pressure: (a) $P_1 = 2.0$ GPa and $P_u = 0.3$ GPa along the [111] axis: intensity of the (101) peak versus temperature showing the Néel transition at 0.7(1) K. (b) $P_1 = 2.4$ GPa and $P_u = 0.3$ GPa along the [011] axis: intensity of the (120) peak versus temperature showing the Néel transition at 1.78(5) K.

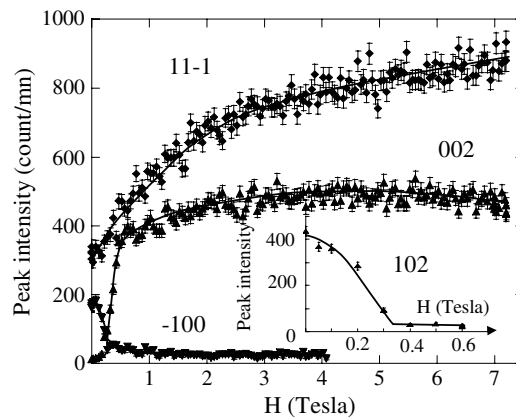


Figure 3. Peak intensity of some typical magnetic peaks versus field H , in the pressure induced ordered state, $P_1 = 2.4$ GPa and $P_u = 0.3$ GPa at $T = 0.14$ K. H and P_u are along the [011] axis.

(above about 6 T). On the assumption of a ferromagnetic-like structure, noticing that the (002) peak is forbidden in the space group $Fd\bar{3}m$, the presence of a magnetic intensity in this peak means that the ferromagnetic component of the ordered moments on the Tb³⁺ sites is non-uniform, even at 7 T.

We have determined the integrated intensity of the magnetic and nuclear peaks at the lowest temperature (0.14 K) for selected field values (0, 0.6 and 4 T) by measuring rocking curves (figure 4(b)). These curves show no appreciable broadening with applied field, and their width remains limited by the experimental resolution. This means that the magnetic phases are long range ordered, with a correlation length above a typical experimental limit of 400 Å. The determination of the integrated intensities allowed us to determine the microscopic spin orientations by refining magnetic models to the data. Within these models, the ordered moments were determined on an absolute scale by calibrating the magnetic peak intensities to the nuclear ones.

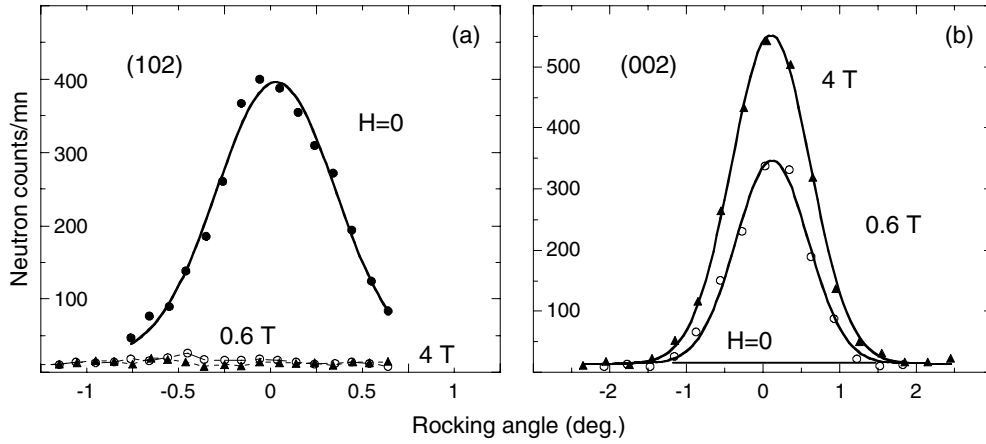


Figure 4. $\text{Tb}_2\text{Ti}_2\text{O}_7$ under pressure and magnetic field H . Magnetic Bragg peaks for several fields in the pressure induced ordered state $P_l = 2.4$ GPa and $P_u = 0.3$ GPa; H and P_u are along the $[011]$ axis. $T = 0.14$ K; $H = 0$ (black dots), 0.6 T (white dots) and 4 T (black triangles).

Table 1. Orientations of the four Tb^{3+} moments in one tetrahedron in the AF structure of figure 5(a), stabilized at $H = 0$, $P_l = 2.4$ GPa, $P_u = 0.3$ GPa along the $[011]$ axis.

Site	x	y	z	Axis
1	0.5	0.5	0.5	$[10\bar{1}]$
2	0.25	0.25	0.5	$[101]$
3	0.25	0.5	0.25	$[\bar{1}01]$
4	0.5	0.25	0.25	$[\bar{1}0\bar{1}]$

5. Microscopic models for the spin correlations

In zero field, we found no intensity in the magnetic peaks corresponding to propagation vectors $\mathbf{k} = (0, 1, 0)$ and $(0, 0, 1)$, which means that the magnetic structure is single \mathbf{k} and develops in a single domain with $\mathbf{k} = (1, 0, 0)$. Similarly, the field induced magnetic structure is a single-domain structure with $\mathbf{k} = 0$. We refined the magnetic structures with the Fullprof program [31]. The cubic cell consists of four Tb^{3+} tetrahedra. In the zero-field $\mathbf{k} = (1, 0, 0)$ AF structure, two tetrahedra have identical and two have reversed spin orientations, whereas in the field induced $\mathbf{k} = 0$ structure, all tetrahedra are identical. To find the local spin structure inside a tetrahedron, we searched for all solutions by simulated annealing (SA) implemented in Fullprof, with the only assumption that of a unique spin length. We also checked for all solutions with $\mathbf{k} = (1, 0, 0)$ described as irreducible representations of the space group $Fd\bar{3}m$, even assuming a non-unique spin length. We found two irreducible representations IR2 with two basic vectors, and two irreducible representations IR4 with four basis vectors. At $H = 0$, the best structure (figure 5(a)), found by SA, has four moments of the same length, oriented along $\langle 101 \rangle$ -type axes, three of them being collinear, with one antiparallel to the others. The moment orientations of the four Tb^{3+} ions are given in the table 1. This structure was already proposed from powder diffraction data. It is close to the structure given by an irreducible representation IR2 with two basic vectors, except that in the IR2 the three collinear moments of the local spin structure are along $[011]$ axes, and not along $[101]$ axes. The only other model found in close agreement with the data ($R_F = 16\%$), is described as an IR4 with four basic

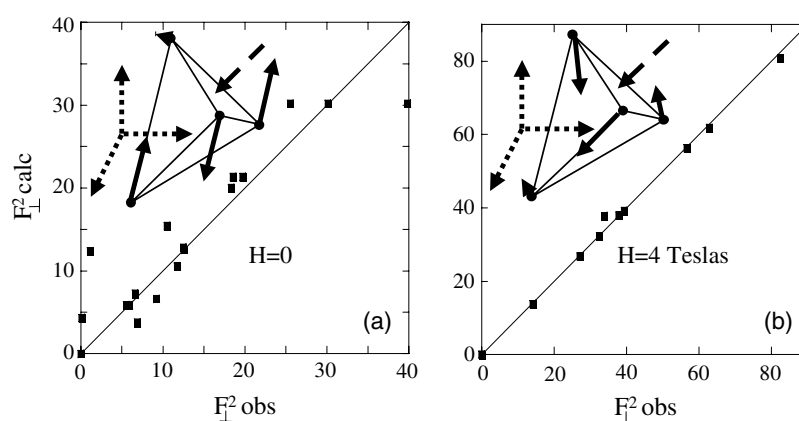


Figure 5. Tb₂Ti₂O₇. Tb₂Ti₂O₇: refined magnetic structure F^2 calc versus F^2 obs, where F^2 is the squared magnetic intensity \perp vector. (a) AF structure at $H = 0$ ($R_F = 14.5\%$). (b) Canted ferromagnetic structure at $H = 4$ T ($R_F = 1.06\%$). In the inset, the local spin structure in one tetrahedron is shown. P_u and H (dashed arrows) are along the [011] axis. At $H = 0$, moments (solid arrows) are along the [101], [10 $\bar{1}$] and [$\bar{1}$ 01] axes; at $H = 4$ T, they make angles varying from 18° to 68° with P_u and H . The principal axes of the cubic cell are indicated by dotted arrows.

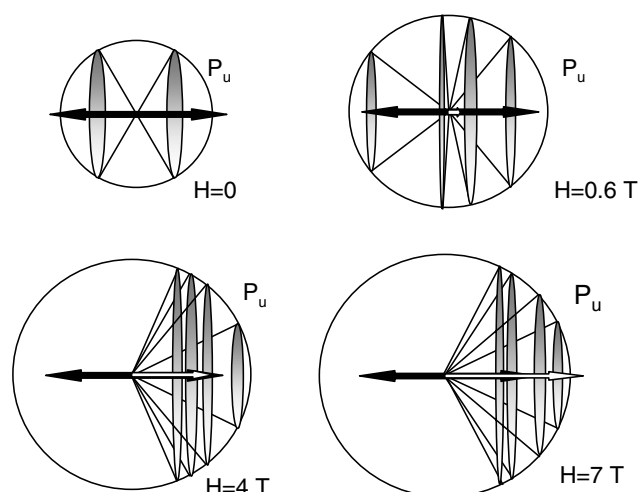


Figure 6. Tb₂Ti₂O₇. Schematic evolution of the local spin structure in one tetrahedron with the magnetic field in the state $P_1 = 2.4$ GPa, $P_u = 0.3$ GPa, $T = 0.14$ K. Black and white arrows refer to the uniaxial pressure P_u and magnetic field H respectively. The cone angles show the orientations of the four Tb³⁺ moments of a given tetrahedron with respect to the field. The radius of a circle is proportional to the ordered moment M_0 .

vectors. It involves two kinds of moments of rather different magnitudes, 4.7(4) and 2.9(6) μ_B respectively, oriented along non-principal directions, and therefore seems to be less likely.

Under an applied field, the local spin structures, found by SA, make some kinds of deformed umbrellas, oriented along the field direction. The best refinement of the structure and the local spin structure is shown for a field of 4 T in figure 5(b). The evolution of the canting angles in one tetrahedron with increasing field are schematized in figure 6. The canting angles slowly decrease with increasing field, but remain far from zero, even at the highest field

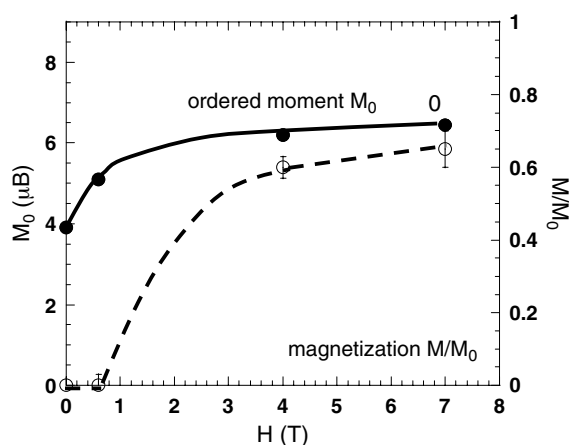


Figure 7. $\text{Tb}_2\text{Ti}_2\text{O}_7$. Variation of the ordered moment M_0 (local Tb^{3+} moment in the AF and canted F ordered structures) and of the net magnetization M (projection of M_0 on the field axis) with the applied field. M_0 and M are deduced from the magnetic refinements. $P_i = 2.4$ GPa, $P_u = 0.3$ GPa along the [011] axis, $T = 0.14$ K.

of 7 T. The evolution of the ordered moment, together with that of the net magnetization (or ferromagnetic component), is plotted in figure 7 versus the applied field. At 4 T, the net magnetization is about 60% of the maximum one and 65% at 7 T. The ordered moment can be calibrated on an absolute scale to $3.9(2) \mu_B$ at $H = 0$, $5.1 \mu_B$ at $H = 0.6$ T and $6.1 \mu_B$ at 4 T. The increase of the ordered moment with the field suggests that at $H = 0$, the ordered structure still coexists with either the spin liquid phase or with another long range ordered, long wavelength modulation. Such modulation was previously observed in the previous powder data, but it could not be checked here.

The evolution of the microscopic spin correlations with the applied field shows that the spin reorientations occur on two different energy scales. A low field of 0.3 T is enough to reorient all tetrahedra in the same direction, yielding the $\mathbf{k} = 0$ structure. In contrast, much stronger fields (evaluated to about 18 T) are needed to suppress the spin canting inside a given tetrahedron. This suggests the existence of two energy scales in the system. A small energy (1 K, 0.6 T) yields the non-frustrated exchange term and induces long range magnetic order. A large energy—of the order of θ_{CW} —needs to overcome the AF exchange interaction to induce full alignment.

6. The magnetic phase diagram in the pressure induced ordered state

By measuring the temperature dependence of the magnetic peaks for different fields (0, 0.6 and 4 T) for given pressure conditions ($P_i = 2.4$ GPa, $P_u = 0.3$ GPa along the [011] axis), we can determine the magnetic phase diagram for these pressures. We observe only one smeared transition towards the paramagnetic phase, where all magnetic peaks disappear. The transition temperature strongly increases with the applied field, by more than one order of magnitude between 0 and 4 T, reaching 23 K at 4 T (figures 8(a) and (b)). We observed thermal irreversibilities at low temperature, with a difference between the zero-field cooled (zfc) and the field cooled (fc) intensities (figure 8(a)). These irreversibilities could be related to the glassy behaviour observed in the magnetization in the same T range at $P = 0$ [22]. The magnetic phase diagram is plotted in figure 9. The large increase of T_N with the applied field

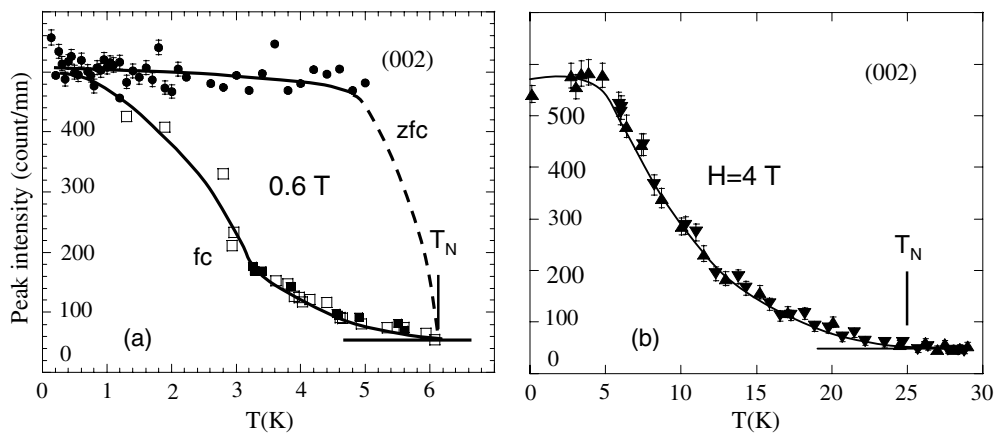


Figure 8. Tb₂Ti₂O₇. Intensity of the (002) magnetic peak versus temperature, in the pressure induced state $P_i = 2.4$ GPa, $P_u = 0.3$ GPa for two applied fields: (a) $H = 0.6$ T; (b) $H = 4$ T. P_u and H are oriented along the [011] axis. Spin glass-like irreversibilities depending on the cooling conditions (zero-field cooling, zfc, or field cooling, fc) are observed at $H = 0.6$ T. The transition temperature T_N strongly increases with the field.

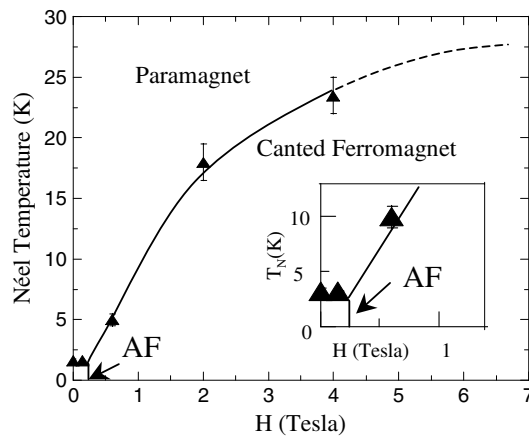


Figure 9. Tb₂Ti₂O₇. The magnetic phase diagram in the pressure induced ordered state $P_i = 2.4$ GPa, $P_u = 0.3$ GPa. P_u and H are oriented along the [011] axis.

in the canted phase suggests that the Zeeman energy dominates the exchange and anisotropy energies. At 4 T, this energy is equal to $\mu H = 33$ K, in the same range as the T_N of 23 K.

7. Discussion

The new single-crystal data are consistent with the previous results on powders, obtained at several pressures in the range 0.15–8.6 GPa. However, in the powders, we could not control the magnitude and orientation of the stress with respect to the crystallites. As shown by the single-crystal data, this is a crucial point for inducing magnetic order. In the powder, a part of the sample could be under a ‘less efficient’ stress, yielding a weaker ordered moment than in the single crystal in the [110] configuration. Another part of the sample could be under the optimal stress, yielding a slightly higher T_N value than in the single crystal (2.1 K instead of 1.8 K).

The single-crystal data give a precise insight into the mechanism which suppresses the spin liquid state in $\text{Tb}_2\text{Ti}_2\text{O}_7$. To understand it, although a microscopic theory is still lacking, one can evaluate the influence of isotropic and anisotropic pressure components on the energy terms. The dipolar energy is smaller than the exchange energy [24], and should not be very sensitive to pressure, since it does not vary strongly with interatomic distances ($E_d \propto r^{-3}$). We estimate that E_d should vary by less than 2% for $P_i = 3$ GPa ($\Delta a/a \sim 0.7\%$). In contrast, superexchange interactions are expected to vary much more with interatomic distances. The strong enhancement of the magnetic fluctuations in the spin liquid state with pressure [27], suggests that this is indeed the case here. The increase in the amplitude of the magnetic fluctuations at 2 K, $I(P = 0)/I(7 \text{ GPa}) = 2.3$, reflects the increase in the thermal average of the magnetic moment squared. From classical molecular field theory, we then evaluate an increase in the exchange energy $E_e = JS^2$ of a factor 1.35 between $P = 0$ and at 7 GPa, that is $\Delta E_e/E_e \Delta P = 0.07 \text{ GPa}^{-1}$. We note that this strong increase is not correlated with an increase in T_N , which remains almost independent of isotropic pressure. Clearly, an isotropic pressure alone cannot change the frustration of the exchange energy term, since it does not affect the lattice symmetry. On the other hand, a T_N value tuned by the stress orientation suggests that geometrical frustration is relieved by a structural distortion, which makes exchange interactions non-equivalent. It should naturally induce a single-domain structure by relieving the cubic degeneracy.

So, we explain our measurements in different pressure configurations as follows. A hydrostatic pressure of 2.8 GPa strongly enhances the exchange interaction (and the Curie–Weiss constant) but does not change the symmetry, so it does not induce magnetic order. On the other hand, a purely uniaxial stress of 0.3 GPa induces uncompensated bonds, but does not strongly modify the exchange interaction, so T_N remains either zero or below our experimental limit (1.4 K in this case). Our recent powder measurements show that the magnetic order could exist on a local scale (about 50 Å) at very low temperature (below 0.3 K), even at zero pressure, probably induced by spontaneous strains. This could also explain the spin glass irreversibilities observed in this T range at ambient pressure. When a uniaxial pressure is applied along the [111] axis, the T_N value and ordered moment remain low, since the stress along [111] does not break the pyramidal symmetry of a Tb^{3+} tetrahedron, and induces few uncompensated bonds. Finally, when combining a hydrostatic pressure with a stress along [110], the optimal orientation for breaking the symmetry and shortening first-neighbour Tb^{3+} bonds selectively, we induce a strong magnetic order.

In this optimal case, we estimate that at $P_u = 0.3$ GPa along [011], a third of the first-neighbour interatomic distances should be compressed by 0.3%, and two thirds should be extended by about 0.1%. Assuming that the increase in the exchange energy comes from the exchange interaction J only, we can evaluate an uncompensated exchange term $\Delta J = 1/3(\Delta J_{011} + \Delta J_{101} + \Delta J_{110})$ as 6% of the frustrated exchange term. By taking into account both the increase in the Curie–Weiss constant due to isotropic pressure (θ_{CW} , estimated in the range [−14 to −11 K] at $P = 0$ [24]), should be enhanced by about 20% at $P_i = 3$ GPa) and the uncompensated exchange, we calculate $T_N = -\theta_{\text{CW}} \Delta J/J$ in the range [1–1.4 K], rather close to the experimental value.

In addition, the stress could also change the local Tb^{3+} moment by changing the symmetry of its oxygen and terbium environment. It could therefore influence the crystal field energy, and possibly relieve the degeneracy of the single-ion ground state. A microscopic theory should take both effects into account, and explain the very strong sensitivity of the exchange energy to interatomic distances. Similar models were proposed for transition metal alloys [32], where the Jahn–Teller effect is higher than in rare earth alloys, with the result that the lattice spontaneously distorts to relieve the frustration (spin–Teller effect).

In spite of a huge theoretical and experimental effort, the stability of the spin liquid state in Tb₂Ti₂O₇ remains a mystery. Showing how to destroy it provides a new insight into this abnormal state. One could propose two scenarios.

- (i) All perturbation terms cancel as for an ideal Heisenberg pyrochlore with first-neighbour interactions only. If so, one could expect a gradual increase of T_N with the magnitude of the stress, or equivalently with the magnitude of the uncompensated exchange interaction.
- (ii) There is a finite window of thermodynamical parameters which stabilize the spin liquid state. This could be the case if quantum fluctuations between the low lying crystal field levels play an important role, as proposed by recent theories [25, 26]. If so, as in liquid helium, one could expect a critical pressure/stress above which the liquid state is destroyed and long range order stabilized.

The magnetic phases observed under field and pressure have the characteristics of standard Néel states. In this respect, they contrast with the field induced phases observed in several pyrochlores [15, 16] and in the low dimensional spin liquid SrCu(BO₃)₂, where non-magnetic sites are created under a field, yielding magnetization plateaus. Could a field alone suppress the liquid phase? This is not clear at present. In Tb₂Ti₂O₇, the magnetic field not only brings in the Zeeman energy, but also distorts the Tb³⁺ lattice by changing the crystal field symmetry, when it does not coincide with the local anisotropy axis. This is at the origin of the giant magnetostriction [23]. According to previous measurements [33], a field of 0.3 T induces an ordered phase with $\mathbf{k} = 0$, which may be similar to the present one. Still, the field induced distortion remains much smaller than the pressure one (typically 0.1 GPa for $H = 7$ T).

In conclusion, by applying a combination of isotropic and anisotropic pressure along the [011] axis of a single crystal of Tb₂Ti₂O₇, we have selectively shortened some of the first-neighbour distances, producing suppression of the spin liquid state and the onset of a complex non-collinear antiferromagnetic phase. Applying in addition a magnetic field induces a second transition towards a canted ferromagnet. The mechanism which relieves the very strong frustration of this compound is now identified, providing a sound basis for further theories.

Acknowledgments

We are very grateful to A Gukasov, responsible for the 6T2 spectrometer, for his long term assistance and support of the experiments. We also thank J M Mignot for his crucial help in cryogenics and J M Mirebeau for a computer program. We thank G Dhalenne and A Revcolevschi for the crystal synthesis, and A Cousson for checking the crystal structure and orientation. In the structural analysis, we benefited from much advice from and illuminating discussions with J Rodríguez-Carvajal, who provided new versions of the programs FullProf and BasIreps. The technical support of P Boutrouille, T Beaufils, J L Meuriot and B Annighöfer is acknowledged.

References

- [1] Grenier B *et al* 2001 *Phys. Rev. Lett.* **86** 5966
Grenier B *et al* 2004 *Phys. Rev. Lett.* **92** 177202
- [2] Collin E *et al* 2001 *Phys. Rev. Lett.* **86** 2447
- [3] Sachdev S 2003 *Rev. Mod. Phys.* **75** 913
- [4] Mila F 2000 *Eur. J. Phys.* **21** 499
- [5] Fouet J B, Mambri M, Zindzinger P and Lhuillier C 2003 *Phys. Rev. B* **67** 54411

- [6] Lauchli A and Poilblanc D 2004 *Phys. Rev. Lett.* **92** 236404
Poilblanc D 2004 *Phys. Rev. Lett.* **93** 197204
- [7] Takada K *et al* 2003 *Nature* **422** 53
- [8] Hanawa M *et al* 2001 *Phys. Rev. Lett.* **87** 187001
- [9] Urano C *et al* 2000 *Phys. Rev. Lett.* **85** 1052
- [10] Reimers J N 1992 *Phys. Rev. B* **45** 7287
- [11] Canals B and Lacroix C 1998 *Phys. Rev. Lett.* **80** 2933
Canals B and Lacroix C 2000 *Phys. Rev. B* **61** 1149
- [12] Lee S H *et al* 2002 *Nature* **418** 856
- [13] Schmidt M *et al* 2004 *Phys. Rev. Lett.* **92** 116401
- [14] Fritsch V *et al* 2004 *Phys. Rev. Lett.* **92** 56402
- [15] Ballou R, Lacroix C and Nunez-Regueiro M D 1991 *Phys. Rev. Lett.* **66** 1910
- [16] Hiroi Z *et al* 2003 *J. Phys. Soc. Japan* **72** 411
- [17] Greedan J E 2001 *J. Mater. Chem.* **37** 11
- [18] Han S W, Gardner J S and Booth C H 2004 *Phys. Rev. B* **69** 24416
- [19] Gardner J S *et al* 1999 *Phys. Rev. Lett.* **82** 1012
Gardner J S *et al* 2001 *Phys. Rev. B* **64** 224416
- [20] Yasui Y *et al* 2002 *J. Phys. Soc. Japan* **71** 599
- [21] Luo G, Hess S T and Corruccini L R 2001 *Phys. Lett. A* **291** 306
- [22] Hamaguchi N, Matsushita T, Wada N, Yasui Y and Masatoshi S 2004 *Phys. Rev. B* **69** 132413
- [23] Alexandrov I V *et al* 1985 *Sov. Phys.—JETP* **62** 1287
- [24] Gingras M J P *et al* 2000 *Phys. Rev. B* **62** 6496
- [25] Kao Y J, Enjalran M, Del Maestro A, Molavian H R and Gingras M J P 2004 *Phys. Rev. B* **68** 172407
- [26] Enjalran M, Scalettar R T and Kauzlarich S M 2004 *J. Phys.: Condens. Matter* **16** S673
- [27] Mirebeau I, Goncharenko I N, Cadavez-Peres P, Bramwell S T, Gingras M J P and Gardner J S 2002 *Nature* **420** 54
- [28] Mirebeau I and Goncharenko I N 2004 *J. Phys.: Condens. Matter* **16** S653
- [29] Mirebeau I, Goncharenko I N, Dhahlenne G and Revcolevschi A 2004 *Phys. Rev. Lett.* **93** 187204
- [30] Goncharenko I N 2004 *High Pressure Res.* **24** 193
- [31] Rodríguez-Carvajal J 1993 *Physica B* **192** 55
- [32] Tchernyshyov O, Moessner R and Sondhi S L 2002 *Phys. Rev. Lett.* **88** 067203
- [33] Yasui Y *et al* 2001 *J. Phys. Chem. Solids* **62** 343